applied sciences

MDPI

Article

Intelligent Position Control for Intelligent Pneumatic Actuator with Ball-Beam (IPABB) System

Mohamed Naji Muftah [1,2], Ahmad Athif Mohd Faudzi [1,3,*], Shafishuhaza Sahlan [1,3] and Shahrol Mohamaddan [4]

[1] Faculty of Electrical Engineering, Universiti Teknologi Malaysia, Skudai, Johor Bahru 81310, Malaysia
[2] Department of Control Engineering, College of Electronics Technology, Bani Walid P.O. Box 38645, Libya
[3] Centre for Artificial Intelligence and Robotics (CAIRO), Universiti Teknologi Malaysia, Jalan Sultan Yahya Petra, Kuala Lumpur 54100, Malaysia
[4] Department of Bioscience and Engineering, College of Systems Engineering and Science, Shibaura Institute of Technology, Saitama 337-8570, Japan
* Correspondence: athif@utm.my

Abstract: A pneumatic actuator system is considered extremely nonlinear, making accurate position control of this actuator difficult to obtain. In this article, a novel cascade fractional-order PID (CFOPID) controller for the intelligent pneumatic actuator (IPA) positioning system utilizing particle swarm optimization (PSO) is presented. The pneumatic system was modeled using the system identification (SI) technique. To demonstrate the effectiveness of the CFOPID controller, a comparison to the FOPID controller is performed based on the rise, settling, and peak times, peak overshoot, and integral of square error (ISE). From the results obtained, the proposed CFOPID controller provides superior control over the FOPID controller. For the application of the position controller, the proposed system incorporates an intelligent pneumatic actuated ball and beam (IPABB) system. The mathematical model of the system was developed and validated through a simulation utilizing a PID (outer loop) and CFOPID controller (inner loop). The suggested controller's accuracy and robustness have been studied by a comparative examination of the results obtained utilizing the proposed and other prior controllers on the same system. The results indicate that the intelligent pneumatic actuator, when coupled with a CFOPID controller, is capable of controlling the positioning of the ball and beam system.

Keywords: intelligent pneumatic actuator; system identification technique; cascade fractional-order proportional–integral–derivative; particle swarm optimization; ball-beam system

Citation: Muftah, M.N.; Faudzi, A.A.M.; Sahlan, S.; Mohamaddan, S. Intelligent Position Control for Intelligent Pneumatic Actuator with Ball-Beam (IPABB) System. *Appl. Sci.* **2022**, *12*, 11089. https://doi.org/10.3390/app122111089

Academic Editor: Oscar Reinoso García

Received: 27 September 2022
Accepted: 31 October 2022
Published: 1 November 2022

1. Introduction

The common application areas of pneumatic systems are mostly in automatic controllers and the automation industry [1]. Pneumatic actuators (PAs) are considered safe and reliable; they are smaller than most other actuators and exhibit high power-to-weight ratios [2]. They have a fast time response and can be used in high-temperature or radioactive situations without causing harm. Pneumatic systems have advantages since gases are not limited by temperature [3–5]. The challenges in controlling PAs are mostly due to the presence of nonlinearities caused by the pneumatic actuator's high friction force, air compressibility, and the valve dead zone [6]. Hence, it is hard to precisely control the PAs.

From the literature [7], there are numerous methods available focusing on improving the performance of pneumatic positioning systems. Many types of linear controllers (such as PID and pole placement) and intelligent controllers (such as neural and fuzzy networks) were researched in the early stages of developing a controller [8].

For example, Faudzi et al. [9] implemented a PI controller on their designed experimental setup while Azman et al. [10] developed a proportional–integral–derivative fuzzy logic (fuzzy-PID) controller. Based on the results of the simulation and the experiments [10],

the fuzzy-PID controller yielded the best performance. A pole-placement feedback control mechanism was presented by Faudzi et al. [11] to control the positioning system of the IPA system. In addition, IPA system position control was achieved by utilizing a generalized predictive controller based on the bat algorithm (GPC-BA), which was developed by Mustafa et al. [12]. The use of a predictive functional controller (PFC) for IPA systems' control was proposed by Osman et al. [13] where a real-time system was developed to validate the results. However, recently, Azira et al. [14] reported that the control of a pneumatic positioning system using the predictive functional controller (PFC) with a novel observer yielded promising results.

In previous decades, due to its increased flexibility in meeting the requirements of specific control applications, numerous research projects have been carried out in fractional-order control (FOC) [15,16]. The FOPID controller, on the other hand, has been applied in diverse areas, such as motor control [17], robotics [18], power systems [19], magnetic levitation systems [20], and time delay systems [21,22]; it also exhibits superior time response attributes when compared to systems using a traditional PID controller. Other research works on FOC include Muftah et al. [23], where a fractional-order PID controller for the IPA positioning system and its performance were compared with a conventional PID controller. In addition, Shouran et al. [24] used fractional-order PID for frequency regulation of a dual-area power system and yielded significant results.

This work is mainly motivated by the need to design and develop a model of the pneumatic system controller. In this work, to obtain the pneumatic system model, the system identification (SI) approach was used. The CFOPID design was used as the new control mechanism for the pneumatic system. To increase the overall system performance, the proposed controller was comprised of an FOPI and was coupled in cascade with an FOPD. Meanwhile, to obtain the best possible design of the CFOPID controller, the PSO method was used by minimizing the time response parameters. The performance of the controller was evaluated using MATLAB simulation, and the results were compared to those obtained using fractional-order proportional–integral–derivative (FOPID). To evaluate the performance of the proposed controllers, a simulated ball and beam system was used. The ball and beam system is considered a model control engineering concept whose fundamental notion can serve in stabilizing a wide range of systems. The ball and beam system is frequently employed mechanically, with a motor, gear, and draw belt, as well as with a servo motor acting as an actuator to control the angle of the beam [25–27]. In this study, an intelligent pneumatic actuator was employed to adjust the angle of the beam, which presents additional challenges for the control system. The system was developed utilizing multiple techniques, including Newton's second law, the Lagrangian method, and conversion to transfer function [25,28]. Newton's second law served as the basis for the development of the mathematical model for describing the dynamic behavior of the proposed system.

This article is organized as follows: Section 2 depicts the dynamic model of the IPA system as well as the ball and beam system. Section 3 discusses the inner loop and outer loop controller designs (PID, FOPID, and CFOPID). Meanwhile, the PSO algorithm is discussed in Section 4. The outcome of the simulation studies for the performance evaluation of the proposed IPA is presented in Section 5, followed by the discussion of the intelligent pneumatic actuated ball and beam system (IPABBS) using FOPID/CFOPID and PID controllers. Finally, Section 6 presents the conclusions.

2. System Modeling

This study focuses on two different design plants, the intelligent pneumatic actuator (IPA) and the ball and beam (BB). The first plant model was created using SI techniques, whereas the second plant model was created through the use of mathematical models. The intelligent pneumatic actuator ball and beam system will be made up of both plants, i.e., IPABBS.

2.1. Modeling of the IPA System

As indicated in Figure 1, the IPA employed in this work consists of five comprehensive components which form an all-in-one actuator system. The five components are optically encoded data, laser stripe code, pressure sensor, programmable system on chip (PSoC) board, and valves. The main benefit of this actuator is its ability to determine the desired output from the feedback inputs through real-time interaction. This actuator features a 0.06 mm laser stripe pitch, a stroke of 200 mm, and a force of 100 N, which allows for providing great accuracy for position control.

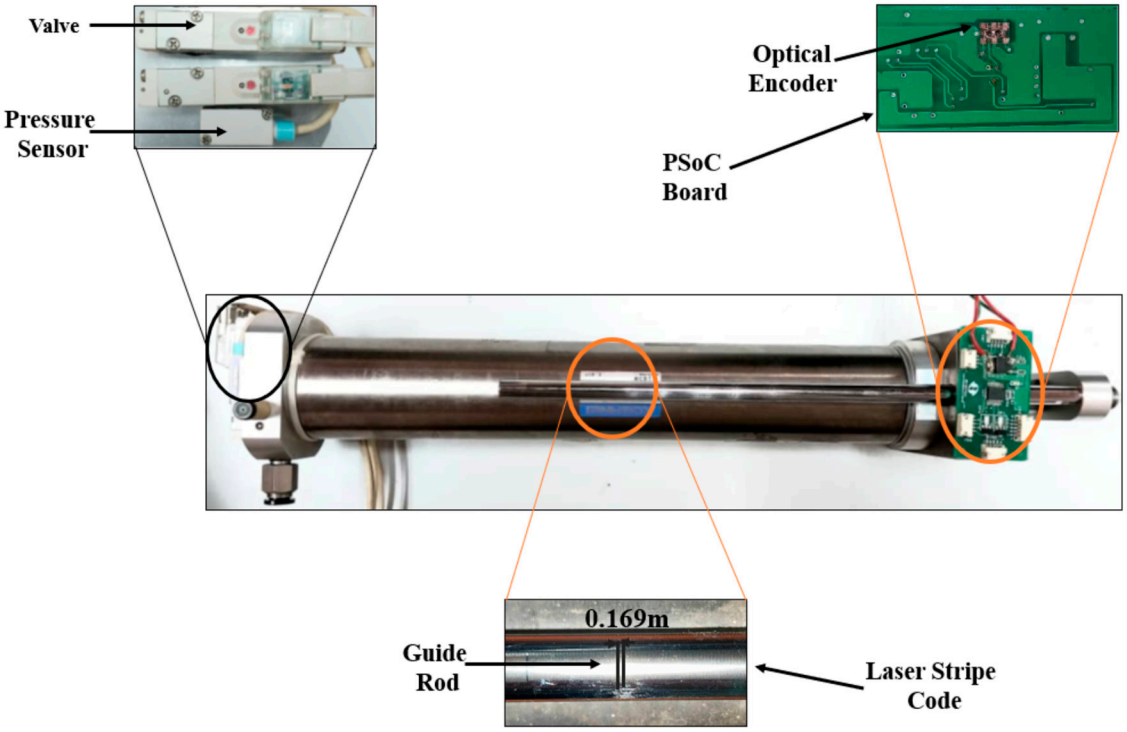

Figure 1. IPA components.

Using a pressure sensor to monitor the cylinder's chamber pressure is an important part of the control process. Driving the cylinder is accomplished by utilizing two on/off valves installed on the cylinder. The PSoC board, which is attached to the top of the actuator, is the central processing unit and it has an optical reflecting surface mount encoder chip. Three components make up this encoder chip: an LED light source, optical lenses, and a photodetector. Table 1 summarizes the cylinder stroke movements based on the valve's conditions.

Table 1. Cylinder stroke movements.

Valve Condition		Cylinder Stroke Motions
V1	**V2**	
OFF	OFF	Stop
OFF	ON	Retract
ON	OFF	Extend
ON	ON	Stop

Figure 2 shows the experimental setup for this work, which includes an SHC68-68-EPM cable, a DAQ card PCI/PXI-6221 (68-Pin) board, and SCB-68 M series devices for connecting the IPA plant to a computer through MATLAB.

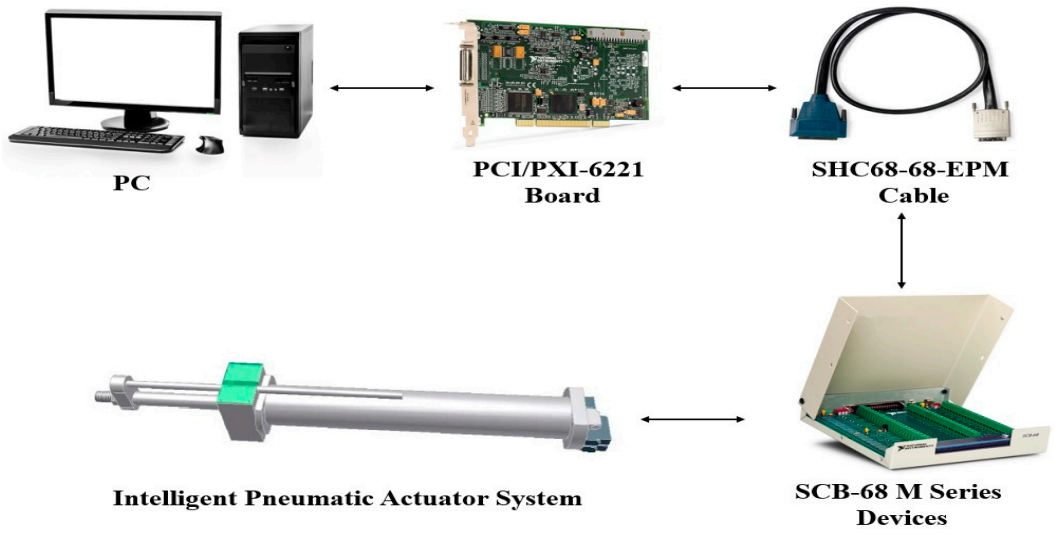

Figure 2. The experimental setup of the system.

The experimental input and output data are utilized to create the mathematical model of the IPA system using the SI approach. A total of 1600 input and output data were collected from a real-time experiment with a sampling time of 0.01 s; 800 samples were used for training, and 800 samples were used for validation. The input and output data from the experiment are plotted in Figure 3.

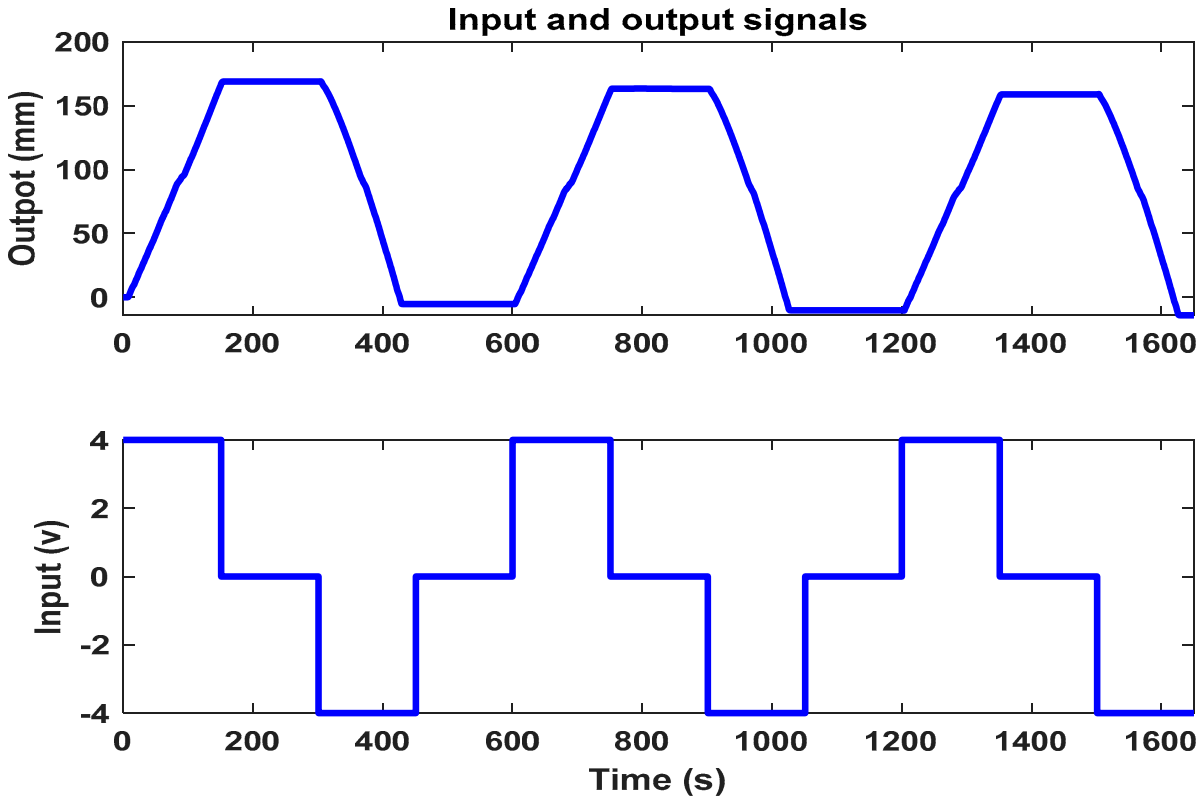

Figure 3. The measured input and output data of the system.

To characterize the dynamic behavior and properties of the IPA system, a parametric model with autoregressive with exogenous input (ARX) was used as the model structure.

Equation (1) describes the discrete ARX transfer function employed in this study. Figure 4 depicts a plot of the output from the measured and simulated models.

$$A = \begin{bmatrix} 2.9900 & -2.9810 & 0.9917 \\ 1 & 0 & 0 \\ 0 & 1 & 0 \end{bmatrix} \quad B = \begin{bmatrix} 1 \\ 0 \\ 0 \end{bmatrix}$$
$$C = \begin{bmatrix} 0.1187 & -0.2350 & 0.1169 \end{bmatrix} \quad D = 0 \tag{1}$$

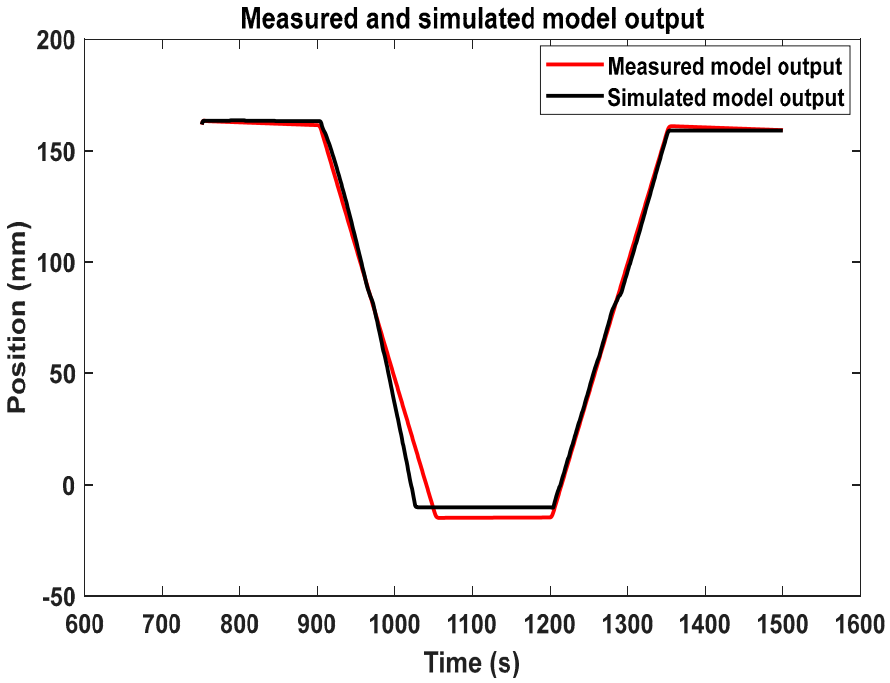

Figure 4. The output of the model, both measured and simulated.

According to Equation (1) and Figure 5, the system is considered stable because all the poles of the system are within the unit circle. In addition, the best fitting criteria of the system is more than 90% after completing the model validation phase in the system identification process.

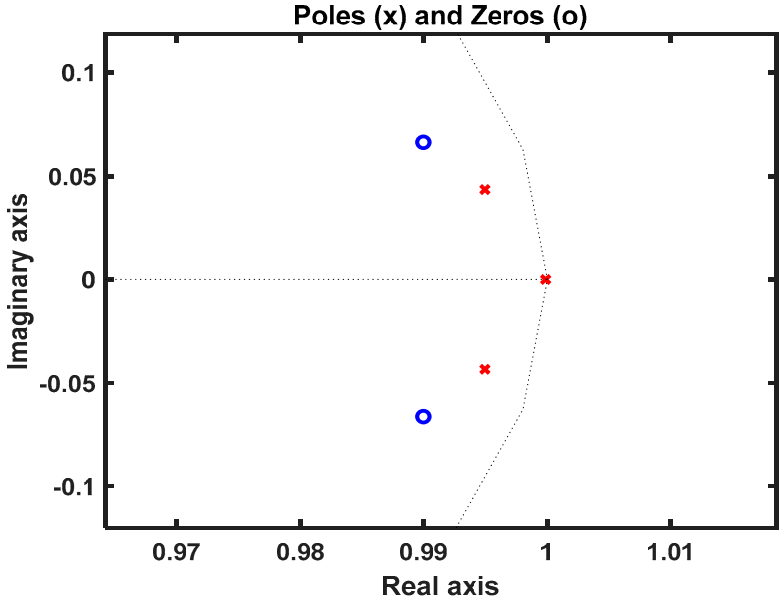

Figure 5. The zero-pole plot for the model.

2.2. Modeling of the Ball and Beam System

The study goal is to provide precise ball position by controlling the stroke length of the IPA. The angle of the beam can be adjusted by moving the pneumatic actuator to keep the ball in a stable state after it has been in an unsteady state. The voltage from the resistance sensor is used to determine the position of the ball, while the position of the encoder is used to determine the angle of the beam, which is dependent on the pneumatic actuator stroke. The ball velocity and acceleration cannot be directly controlled easily due to the existing friction coefficient between the beam and the ball; similarly, it is not easy to directly control the PA stroke due to its nonlinearity.

To construct a suitable controller for this system, it is important to derive the system dynamics equation. As illustrated in Figure 6, the beam is moved vertically (y-axis) by delivering torque from the right pneumatic actuator to the pivot at the left end. The ball is moved along the horizontal axis (x-axis) by the movement of the beam up and down.

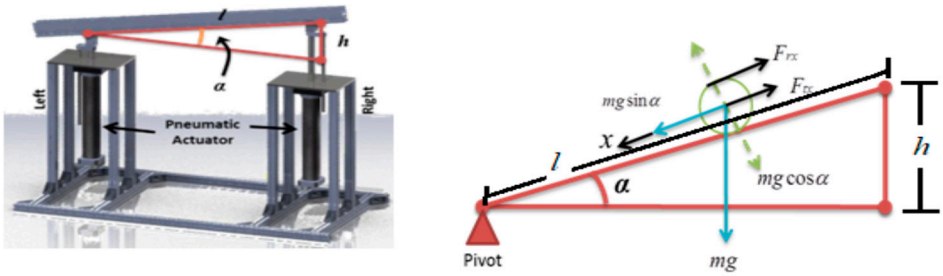

(**a**) (**b**)

Figure 6. (**a**) IPABB system (**b**) Free body diagram.

To simplify and linearize the model, all friction forces are ignored; the ball and the beam are always in contact, and there is no slippage when the ball is rolling on the beam. Table 2 presents the suggested system parameters.

Table 2. IPABB system parameters.

Quantity	Value
Beam Length (l)	0.5 m
Pneumatic Actuator Stroke Length (h)	0–200 mm
Angle (α)	Depends on h
The Ball Mass (m)	0.04012 kg
The Ball Radius (R)	0.0107 m
Ball's Moment of Inertia (J)	1.8373×10^{-6}
Gravitational Acceleration (g)	9.8 ms^{-2}

Newton's second law of motion is used to figure out the nonlinear mathematical description of the system. The system has two forces: a translational force (F_{tx}) that acts under gravity in the x-direction, and a rotating force (F_{rx}) caused by the torque from the rotational acceleration of the ball.

Figure 6b illustrates the free-body depiction of the acceleration $\frac{d^2x}{dt^2}$ along x as $\ddot{x}$, which corresponds to the force owing to translational motion as presented in Equation (2).

$$F_{tx} = m\ddot{x} \tag{2}$$

The torque generated by the spinning of the ball can be expressed as follows:

$$T_r = F_{rx}\, R = J\frac{dw_b}{dt} = J\frac{d\left(\frac{v_b}{R}\right)}{dt} = J\frac{d^2\left(\frac{x}{R}\right)}{dt^2} = \frac{J}{R}\ddot{x} \tag{3}$$

where R is the radius of the ball.

Equation (3) can so be restructured to provide the following:

$$F_{rx} = \frac{J}{R^2}\ddot{x} \tag{4}$$

where J denotes the moment of inertia of the ball, which can be expressed as Equation (5).

$$J = \frac{2}{5}mR^2 \tag{5}$$

Substituting Equation (5) into Equation (4) provides Equation (6):

$$F_{rx} = \frac{2}{5}m\ddot{x} \tag{6}$$

When Newton's second law is applied to forces along an incline, Equation (7) is obtained:

$$F_{rx} + F_{tx} = mg\ \sin\ \alpha \tag{7}$$

In Equation (7), m denotes the mass of the ball, g is the acceleration due to gravity, and α denotes the angle of the beam. Equation (8) is obtained by substituting Equation (2) and Equation (6) into Equation (7).

$$\frac{2}{5}m\ddot{x} + m\ddot{x} = mg\sin\alpha \tag{8}$$

Equation (8) can be restructured to provide Equation (9).

$$\ddot{x} = \frac{5}{7}\,g\sin\alpha \tag{9}$$

The beam angle, α as shown in Equation (9) for the suggested ball and beam system is determined by the pneumatic actuator stroke length, h. We can represent the beam angle in the following way based on Figure 6a:

$$\alpha = \sin^{-1}\frac{h}{l} \tag{10}$$

where l represents the beam length.

3. Controller Design

The design of the controllers for the IPA plant, as well as the ball and beam plant, are discussed in this section. The control system design for the proposed system necessitates two feedback loops, one for the IPA (inner loop) and one for ball position control (outer loop). The inner loop, C2, controls the length of the pneumatic stroke, h, which drives the beam (controls the angle, α). It is required that this inner loop controller should be designed to accurately control the position of the IPA. The outer loop, C1, controls the position of the ball using the inner feedback loop.

3.1. Control of IPA System (Inner Loop)

3.1.1. The Fractional-Order PID (FOPID) Controller

Industrial control systems commonly use a PID controller, which has been extended to include a fractional-order version called the fractional-order PID (FOPID) controller. The fractional PID was first introduced in 1994, and since then, it has achieved a significant position as a robot controller [29]. One of the most evident reasons for its widespread use is owing to its straightforward design and good performance, which includes a quick response with a low overshoot percentage even in the case of slow regulated plants [30]. The FOPID controller seeks to rectify the difference between the desired setpoint and a measured

process variable by calculating and displaying a corrective action that can be used to change the process. The following is a description of the FOPID controller's transfer function [31]:

$$C2(s) = \frac{U(s)}{E(s)} = K_p + \frac{K_i}{S^{\lambda}} + K_d S^{\mu} \quad (11)$$

The FOPID equation includes five unknown parameters, where K_p is the proportional gain, K_i is the integral gain, K_d is the derivative gain, λ is the fractional-order integral, and μ is the fractional-order derivative. Figure 7 illustrates the structure of an FOPID controller.

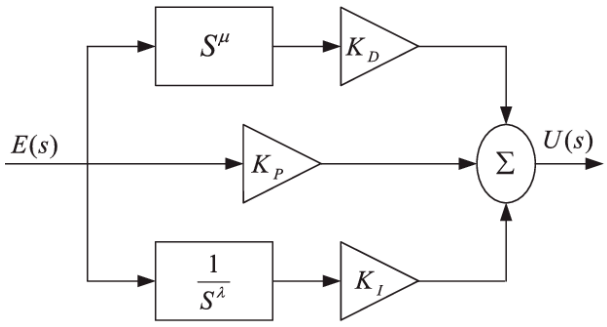

Figure 7. The FOPID controller structure.

As illustrated in Figure 8, the FOPID controller is represented graphically by an order of integrator and a differentiator with an *x*-axis representing the integrator and a *y*-axis representing the differentiator. The values of μ and λ determine how well the traditional P, PI, PD, and PID controllers can be derived from the FOPID controller.

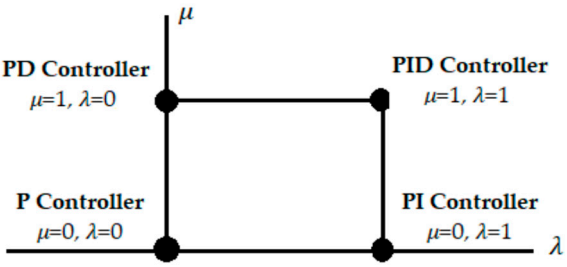

Figure 8. Graphical representation of FOPID controller.

3.1.2. The Cascade Fractional-Order PID (CFOPID) Controller

The CFOPID structure described in this paper is depicted in Figure 9. The suggested structure is made up of two controllers, PI^{λ} and PD^{μ}, which are connected in a cascade. Equation (12) expresses the system's control signal:

$$C2(s) = \frac{U(s)}{E(s)} = \left(K_p + \frac{K_i}{S^{\lambda}}\right) \cdot \left(K_{p1} + K_d S^{\mu}\right) \quad (12)$$

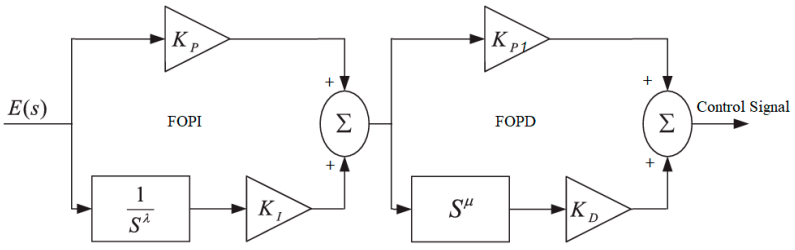

Figure 9. The CFOPID controller structure.

This controller's performance must be optimized to improve transient responsiveness while also minimizing error. Six parameters must be modified in order to achieve this goal: K_p, K_i, K_d, K_{p1}, λ, and μ.

3.2. Control of the Ball and Beam System (Outer Loop)

The ball position is controlled by the outer loop, which uses a PID controller to adjust the angle of the beam. Figure 10 illustrates the PID controller's construction. The transfer function of PID control is shown in Equation (13):

$$C1(s) = \frac{U(s)}{E(s)} = K_p + \frac{K_i}{S} + K_d S \quad (13)$$

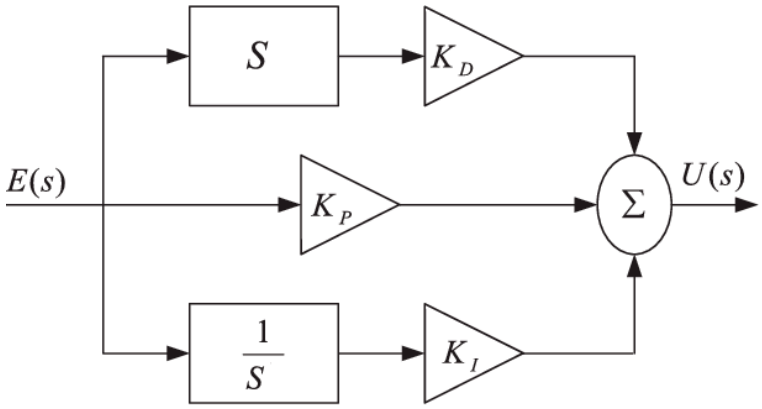

Figure 10. The PID controller structure.

4. Particle Swarm Optimization Algorithm

James and Russell introduced particle swarm optimization in 1995 [32] as a random probability distribution search method inspired by the flocking patterns of birds [33]. It is a very effective optimization tool that has been found useful in solving problems that are not linearly optimal [22,34]. In 1998, an upgraded PSO was introduced to improve the performance of the conventional PSO. Inertia weight was added as an additional coefficient to the extended PSO. PSO was developed as a set of rules that correlate the birds' cognition with their ability to collaborate in a public setting. With this method, each bird (particle) seeks the optimal position by updating its current location in the swarm by exploiting its memory of the best-found position and knowledge of the global best location [34].

The specific steps of the process of the standard PSO algorithm are shown in the flowchart (Figure 11).

The integral absolute errors (IAE), the integral of square errors (ISE), and the integral of time square errors (ITSE) are three common fitness metrics used to assess system performance in optimization strategies [35]. In this study, the ISE fitness function, shown in Equation (14), is used as a measure of how well the output response of the system works:

$$ISE = \int_0^t e(t)^2.dt \quad (14)$$

Table 3 summarizes the parameters of the PSO algorithm used in this study.

Table 3. The parameters of PSO.

Parameter	No. Iteration	No. Particles	Social-Coefficient (s)	Cognitive-Coefficient (c)	Inertia-Weight (iw)
Value	30	10	1.42	1.42	0.9

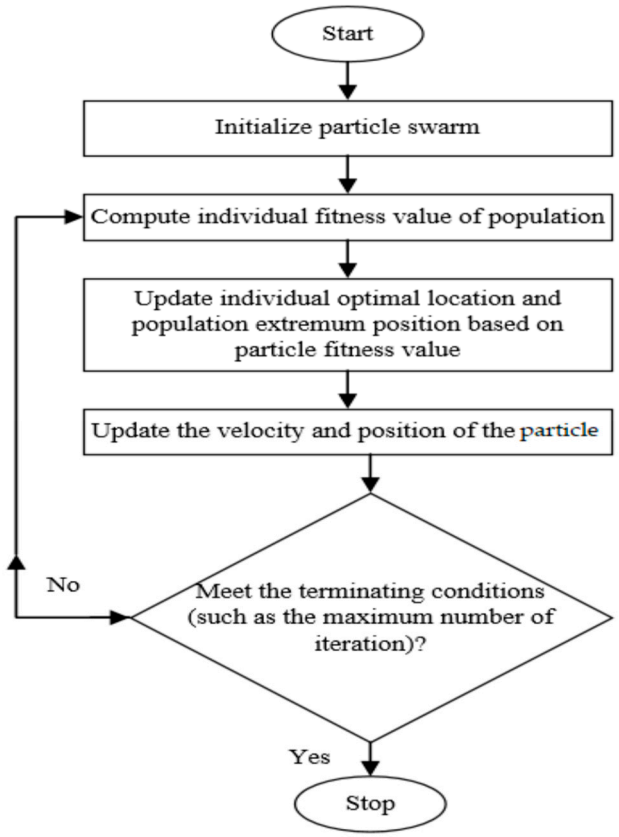

Figure 11. Flowchart of the standard PSO algorithm.

5. Results and Discussion

To improve the precision and accuracy of the pneumatic actuator's cylinder stroke while maintaining the appropriate position, a CFOPID controller was tested in SIMULINK, as illustrated in Figure 12. As a result, the suggested controller improved the transient responsiveness while minimizing the system's overall performance overshoot, rise time, and settling time. Comparisons were made between the performance of the proposed controller and the FOPID controller, which was also tested.

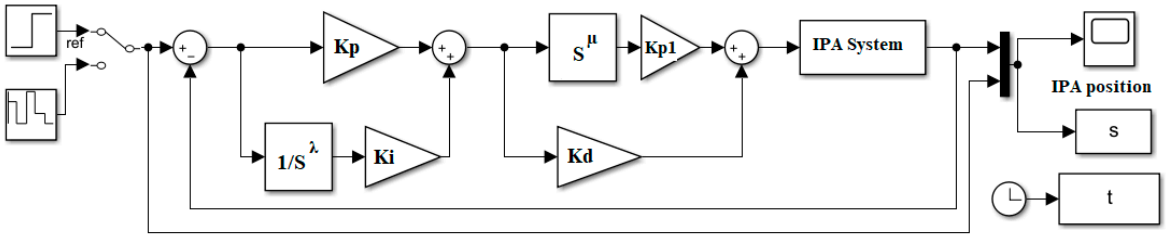

Figure 12. Simulink diagram for simulation CFOPID.

As determined by PSO, Table 4 provides a summary of the optimal parameter values for both the CFOPID and the FOPID controllers.

Table 4. The optimal values of the controllers.

Criteria	K_p	K_i	λ	K_d	μ	K_p1
CFOPID	50	48.6378	1.0141	50	0.25	39.8685
FOPID	50	50	0.817	50	0.25	-

Table 5 shows a summary of how well the CFOPID and FOPID controllers worked. In this research, controllers were ranked according to how well they managed the IPA positioning system. The CFOPID model that was optimized using PSO yielded the best results in terms of performance (Ts, Tr, and OS%).

Table 5. The optimal values of the CFOPID and FOPID controllers.

Criteria	Tr (s)	Ts (s)	OS%	ISE
CFOPID	0.008	0.0098	0.1587	0.0001205
FOPID	0.0133	0.0510	1.1619	0.002699

Figure 13 shows a comparison of the CFOPID and FOPID controllers' responses, revealing that the CFOPID controller results in a significantly lower overshot (OS%) in the system response (at 0.1587) compared to the FOPID controller (at 1.1619). Furthermore, in terms of reference signal tracking, the CFOPID beats all other controllers evaluated in this study.

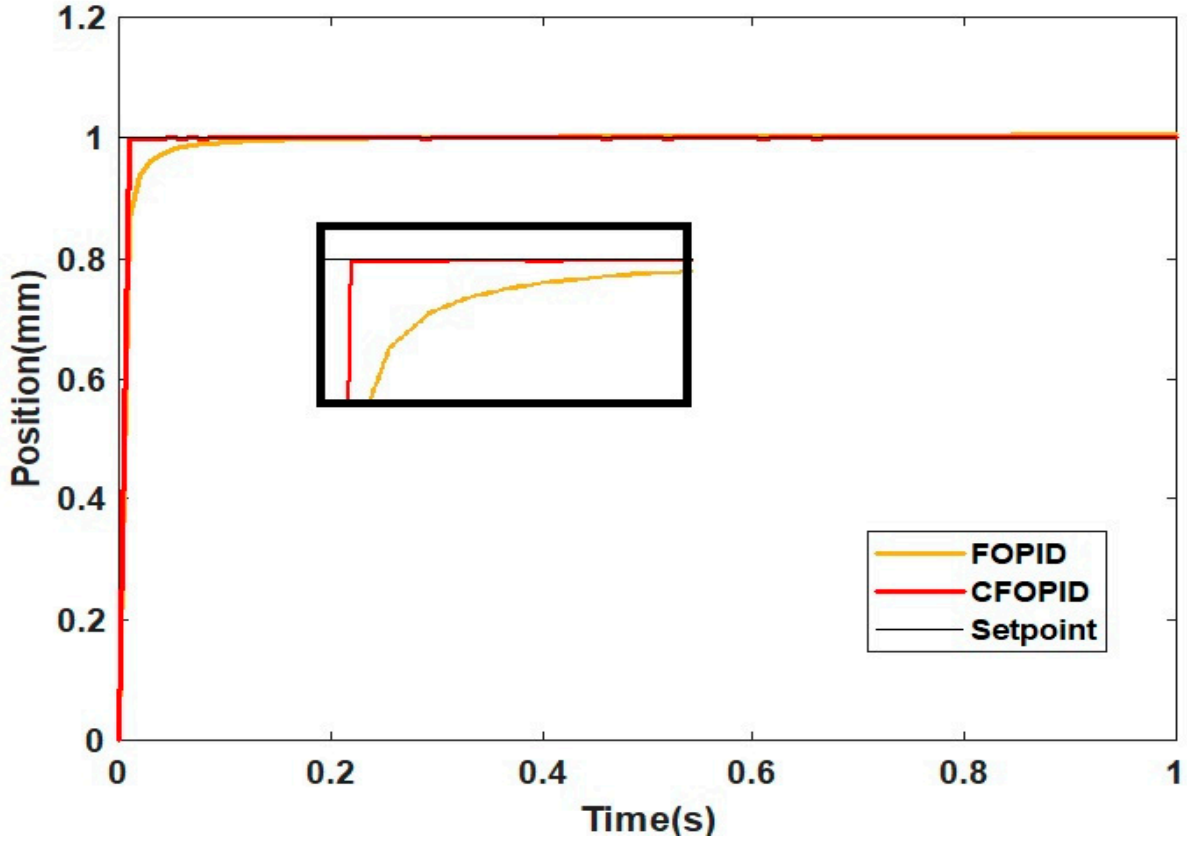

Figure 13. The responses of CFOPID and FOPID controllers.

The performance of the suggested controller can be assessed by applying a varying setpoint to its input. A comparison of the capabilities of CFOPID controllers and FOPID controllers is presented in Figure 14. This unequivocally demonstrates that the CFOPID controller was superior to the FOPID controller in terms of performance. A significant improvement has been made to the CFOPID controller's trajectory tracking capacity, and several performance indicators have been improved as well, including the transient response of the system.

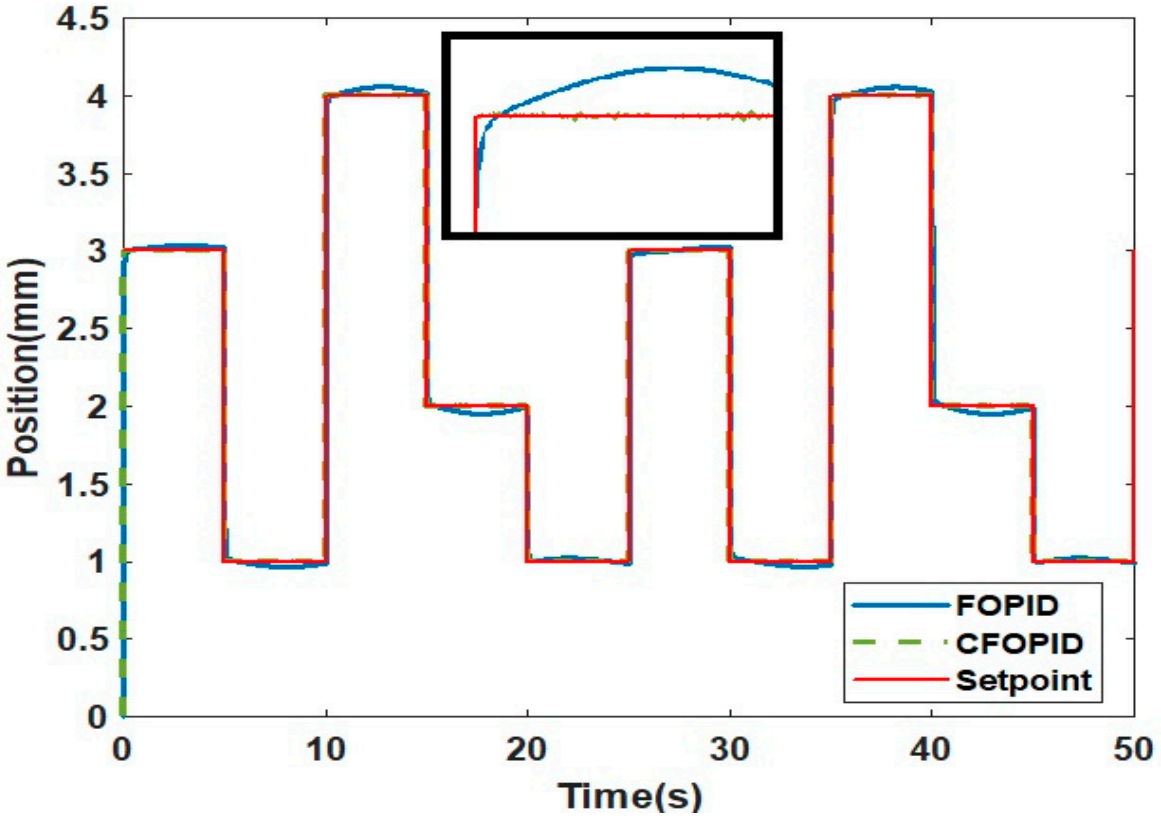

Figure 14. The CFOPID and FOPID controllers' responses with varying setpoint.

Additionally, the outcomes are contrasted with those from studies that used the generalized predictive controller (GPC) presented in [36], the model predictive controller (MPC) presented in [37], and the predictive functional controller (PFC) with the novel observer method presented in [14] for the same system in order to show the superiority of the CFOPID controller. Table 6 displays the results obtained from using these controllers.

Table 6. Comparison between the CFOPID and other controllers' performance.

Criteria	Tr (s)	Ts (s)	OS%
CFOPID	0.008	0.0098	0.1587
FOPID	0.0133	0.0510	1.1619
GPC [36]	0.165	0.25	0.7
MPC [37]	0.5330	0.7331	0.0122
PFC-O [14]	0.5665	0.8166	≈0

Table 6 gives more evidence that the controller that is being presented is superior to those that have been proposed in earlier publications. In comparison to the methods examined in [14,36,37], the settling time and rise time are found to be shorter when employing the suggested CFOPID controller. Nonetheless, a slight increase in the overshoot is observed.

The ability to control a ball for the IPABB system is demonstrated by the analytical findings for position tracking of a pneumatic actuator. The CFOPID controller was chosen as the inner loop control because it has a good and reliable response. The outer loop controller is a PID controller, as detailed in Section 3. The PSO algorithm can be used to tune the values of a PID controller. The gains values are: K_p = 10, K_i = 1, and K_d = 50.

The block diagram of the IPABB system is shown in Figure 15. CFOPID (inner loop) and PID (outer loop) were used to simulate ball position for step and multistep responses. The pneumatic actuator stroke position is shown in Figures 16 and 17 as a step and multistep reaction to the ball position. Furthermore, as previously stated, the findings of the suggested

inner and outer loop controllers are compared to the previously published study for the identical system in [28].

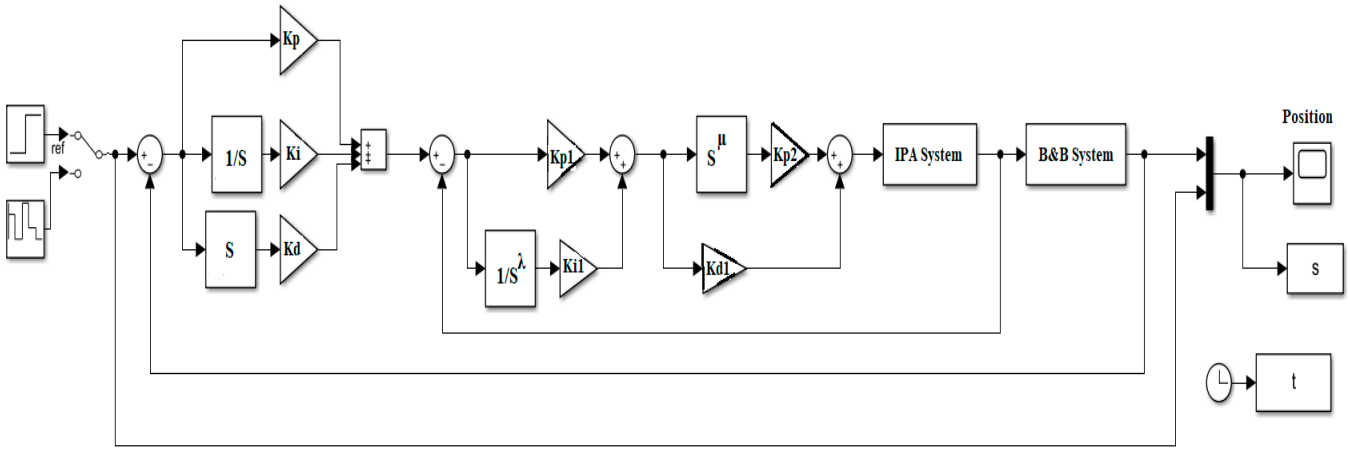

Figure 15. Simulink diagram for simulation IPABB system.

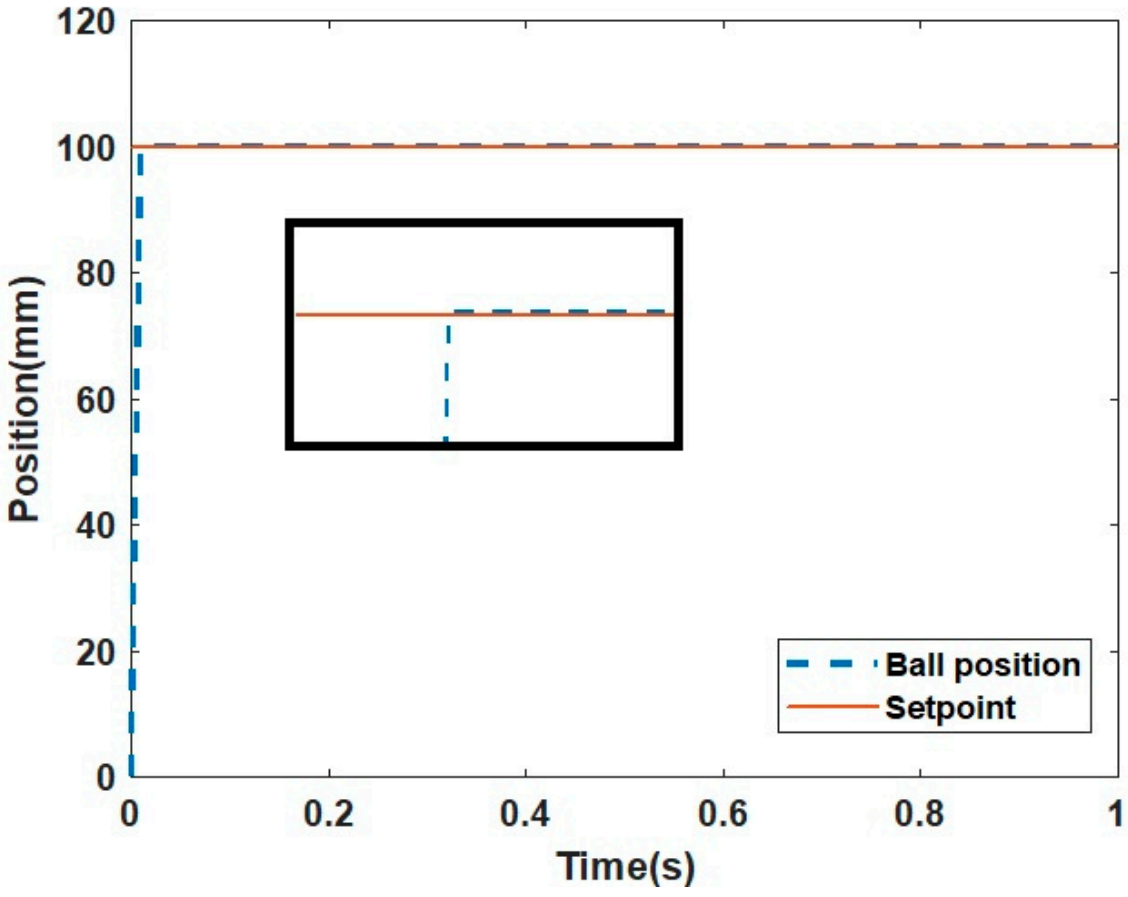

Figure 16. The responses of CFOPID and PID controllers.

The dynamic performance of the IPABBS based on the CFOPID controller (inner loop), and the PID controller (outer loop) both tuned using the PSO algorithm, represented by rise time, settling time, peak overshoot, and ISE is illustrated in Table 7. The IPABBS's performance demonstrates that the controller design is appropriate for the intended system.

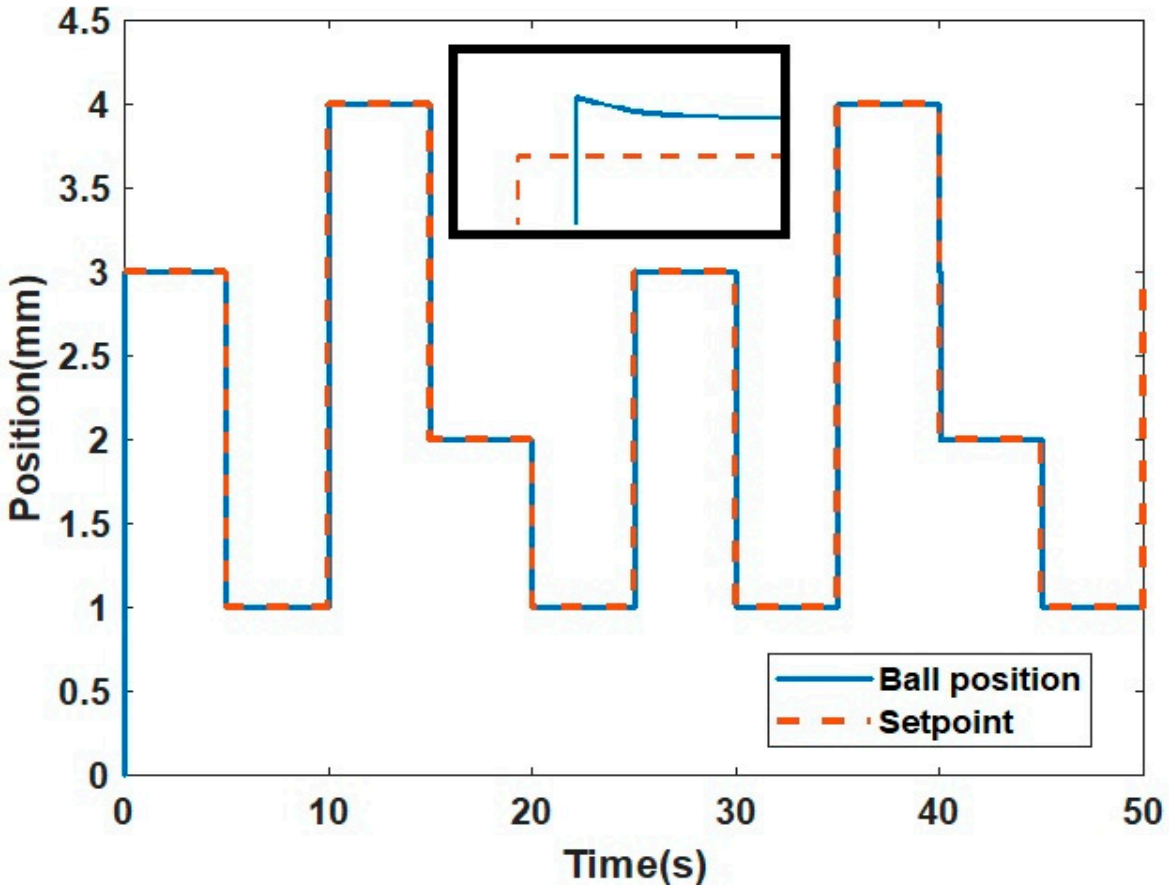

Figure 17. The CFOPID and PID controllers' responses with varying setpoint.

Table 7. The optimal values of the CFOPID and FOPID controllers.

Controller		Tr (s)	Ts (s)	OS%	ISE
Inner Loop	**Outer Loop**				
PID	CFOPID	0.008	0.0098	0.0307	0.0005507
PD-Fuzzy [28]	Feedback control [28]	0.9498	1.72	0	191.413

6. Conclusions

This work presented the modeling and position control of an intelligent pneumatic actuator (IPA) system. The system identification approach based on an auto-regressive with exogenous input (ARX) model was used for the pneumatic system modeling. In the meantime, a developed cascade fractional-order PID (CFOPID) was applied to the system in order to guarantee accurate positional control compared to the FOPID. The results confirmed that the CFOPID controller outperforms FOPID due to its superior robustness, stability, fast reaction, and zero steady-state error. In order to stabilize the ball at the desired position, the model and controller of the pneumatic actuator were utilized to develop the model and construct the controllers for the intelligent pneumatic actuated ball and beam (IPABB) system. This plant was controlled by two control loops, the inner loop for positioning the pneumatic actuator and the outside loop for positioning the ball along the beam. Finally, the simulation results show that, in comparison to other controllers, the CFOPID (inner loop controller) with PID (outer loop controller) provide a quick and smooth response for managing the motion of the ball. For future work, the proposed controller will be tested in a real-time experiment to validate its performance in pneumatic positioning control and positioning the ball along the beam.

Author Contributions: Conceptualization, M.N.M.; Data curation, M.N.M.; Formal analysis, M.N.M.; Funding acquisition, M.N.M. and A.A.M.F.; Investigation, M.N.M.; Methodology, M.N.M., A.A.M.F., S.S. and S.M.; Project administration, M.N.M., A.A.M.F., S.S. and S.M.; Resources, M.N.M., A.A.M.F., S.S. and S.M.; Software, M.N.M., A.A.M.F. and S.S.; Supervision, A.A.M.F., S.S. and S.M.; Validation, M.N.M.; Visualization, M.N.M. and S.S.; Writing—original draft, M.N.M.; Writing—review & editing, M.N.M., A.A.M.F., S.S. and S.M. All authors have read and agreed to the published version of the manuscript.

Funding: This research received no external funding.

Institutional Review Board Statement: Not applicable.

Informed Consent Statement: Not applicable.

Data Availability Statement: Not applicable.

Acknowledgments: The research has been carried out under the program Research Excellence Consortium (JPT (BPKI) 1000/016/018/25 (57)) with the title Consortium of Robotics Technology for Search and Rescue Operations (CORTESRO) provided by the Ministry of Higher Education Malaysia (MOHE). The authors also acknowledge Universiti Teknologi Malaysia (UTM) under vote no (4L930) for the facilities and support to complete this research.

Conflicts of Interest: The authors declare no conflict of interest.

References

1. Qian, P.; Pu, C.; Liu, L.; Lv, P.; Ruiz Páez, L.M. A novel pneumatic actuator based on high-frequency longitudinal vibration friction reduction. *Sens. Actuators A Phys.* **2022**, *344*, 113731. [CrossRef]
2. Ren, H.P.; Fan, J.T.; Kaynak, O. Optimal Design of a Fractional-Order Proportional-Integer-Differential Controller for a Pneumatic Position Servo System. *IEEE Trans. Ind. Electron.* **2019**, *66*, 6220–6229. [CrossRef]
3. Muftah, M.N.; Xuan, W.L.; Athif, A.; Faudzi, M. ARX, ARMAX, Box-Jenkins, Output-Error, and Hammerstein Models for Modeling Intelligent Pneumatic Actuator (IPA) System. *J. Integr. Adv. Eng.* **2021**, *1*, 81–88. [CrossRef]
4. Faudzi, A.À.M.; Suzumori, K.; Wakimoto, S. Development of Pneumatic Actuated Seating System to aid chair design. In Proceedings of the 2010 IEEE/ASME International Conference on Advanced Intelligent Mechatronics, Montreal, QC, Canada, 6–9 July 2010.
5. Sulaiman, S.F.; Rahmat, M.F.; Faudzi, A.A.; Osman, K.; Samsudin, S.I.; Abidin, A.F.Z.; Sulaiman, N.A. Pneumatic positioning control system using constrained model predictive controller: Experimental repeatability test. *Int. J. Electr. Comput. Eng. IJECE* **2021**, *11*, 3913–3923. [CrossRef]
6. Faudzi, A.M.; Osman, K.; Rahmat, M.F.; Mustafa, N.D.; Azman, M.A.; Suzumori, K. Nonlinear mathematical model of an Intelligent Pneumatic Actuator (IPA) systems: Position and force controls. In Proceedings of the 2012 IEEE/ASME International Conference on Advanced Intelligent Mechatronics (AIM), Kaohsiung, Taiwan, 11–14 July 2012; pp. 1105–1110. [CrossRef]
7. Bone, G.M.; Xue, M.; Flett, J. *Position Control of Hybrid Pneumatic-Electric Actuators Using Discrete-Valued Model-Predictive Control*; Mechatronics. Elsevier Ltd.: Amsterdam, The Netherlands, 2015; pp. 1–10.
8. Mu, S.; Goto, S.; Shibata, S.; Yamamoto, T. Intelligent position control for pneumatic servo system based on predictive fuzzy control. In *Computers and Electrical Engineering*; Elsevier Ltd.: Amsterdam, The Netherlands, 2019; pp. 112–122.
9. Faudzi, A.A.M.; Suzumori, K.; Wakimoto, S. Development of an intelligent pneumatic cylinder for distributed physical human-machine interaction. *Adv. Robot.* **2009**, *23*, 203–225. [CrossRef]
10. Azman, M.A.; Faudzi, A.'A.M.; Elnimair, M.O.; Hikmat, O.F.; Osman, K.; Kai, C.C. P-Adaptive Neuro-Fuzzy and PD-Fuzzy controller design for position control of a modified single acting pneumatic cylinder. In Proceedings of the 2013 IEEE/ASME International Conference on Advanced Intelligent Mechatronics, Wollongong, Australia, 9–12 July 2013; pp. 176–181. [CrossRef]
11. Faudzi, A.M.; Mustafa, N.D.; bin Osman, K.; Azman, M.A.; Suzumori, K. GPC controller design for an Intelligent Pneumatic Actuator. *Procedia Eng.* **2012**, *41*, 657–663. [CrossRef]
12. Mustafa, N.D.; Faudzi, A.A.M.; Abidin, A.F.Z.; Osman, K.; Suzumori, K. Generalized predictive controller using Bat algorithm for double acting pneumatic cylinder. In Proceedings of the 2013 IEEE Student Conference on Research and Development, Putrajaya, Malaysia, 16–17 December 2013; pp. 572–576. [CrossRef]
13. Osman, K.; Faudzi, A.'A.M.; Rahmat, M.F.; Hikmat, O.F.; Suzumori, K. Predictive Functional Control with Observer (PFC-O) Design and Loading Effects Performance for a Pneumatic System. *Arab. J. Sci. Eng.* **2014**, *40*, 633–643. [CrossRef]
14. Azira, A.R.; Osman, K.; Samsudin, S.I.; Fatimah Sulaiman, S. Predictive Functional Controller (PFC) with Novel Observer Method for Pneumatic Positioning System. *J. Telecommun. Electron. Comput. Eng.* **2018**, *10*, 119–124.
15. Muftah, M.N.; Faudzi, A.A.M. Tracking Performance of Pneumatic Position Using Fractional-Order PI λ D μ Controller. *Mater. Sci. Eng.* **2021**, *1153*, 012011. [CrossRef]
16. Sikander, A.; Thakur, P.; Bansal, R.; Rajasekar, S. A novel technique to design cuckoo search based FOPID controller for AVR in power systems. *Comput. Electr. Eng.* **2018**, *70*, 261–274. [CrossRef]

17. Rajasekhar, A.; Jatoth, R.K.; Abraham, A. Design of intelligent PID/PIλDμ speed controller for chopper fed DC motor drive using opposition based artificial bee colony algorithm. *Eng. Appl. Artif. Intell.* **2014**, *29*, 13–32. [CrossRef]
18. Dumlu, A.; Erenturk, K. Trajectory Tracking Control for a 3-DOF Parallel Manipulator Using Fractional-Order Control. *IEEE Trans. Ind. Electron.* **2013**, *61*, 3417–3426. [CrossRef]
19. Mishra, A.K.; Das, S.R.; Ray, P.K.; Mallick, R.K.; Mohanty, A.; Mishra, D.K. PSO-GWO Optimized Fractional Order PID Based Hybrid Shunt Active Power Filter for Power Quality Improvements. *IEEE Access* **2020**, *8*, 74497–74512. [CrossRef]
20. Asif, H.; Nasir, A.; Shami, U.T.; Rizvi, S.T.H.; Gulzar, M.M. Design and comparison of linear feedback control laws for inverse Kinematics based robotic arm. In Proceedings of the 2017 13th International Conference on Emerging Technologies (ICET), Islamabad, Pakistan, 27–28 December 2017. [CrossRef]
21. Luo, Y.; Chen, Y. Stabilizing and robust fractional order PI controller synthesis for first order plus time delay systems. *Automatica* **2012**, *48*, 2159–2167. [CrossRef]
22. Bingul, Z.; Karahan, O. Comparison of PID and FOPID controllers tuned by PSO and ABC algorithms for unstable and integrating systems with time delay. *Optim. Control Appl. Methods* **2018**, *39*, 1431–1450. [CrossRef]
23. Muftah, M.N.; Mohd Faudzi, A.A. *Fractional-Order PIλDμ Controller for Position Control of Intelligent Pneumatic Actuator (IPA) System*; Springer: Singapore, 2021.
24. Shouran, M.; Alsseid, A. Particle Swarm Optimization Algorithm-Tuned Fuzzy Cascade Fractional Order PI-Fractional Order PD for Frequency Regulation of Dual-Area Power System. *Processes* **2022**, *10*, 477. [CrossRef]
25. Nguyen, C.X.; Phan, H.N.; Hoang, L.D.; Tran, H.N. The design of a quasi-time optimal cascade controller for ball and beam system. *IOP Conf. Ser. Mater. Sci. Eng.* **2021**, *1029*, 012022. [CrossRef]
26. Mehedi, I.M.; Al-Saggaf, U.M.; Mansouri, R.; Bettayeb, M. Two degrees of freedom fractional controller design: Application to the ball and beam system. *Measurement* **2018**, *135*, 13–22. [CrossRef]
27. Šitum, Ž.; Trslić, P. Ball and beam balancing mechanism actuated with pneumatic artificial muscles. *J. Mech. Robot.* **2018**, *10*, 1–7. [CrossRef]
28. Azman, M.A.; Osman, K.; Natarajan, E. Integrating servo-pneumatic actuator with ball beam system based on intelligent position control. *J. Teknol.* **2014**, *69*, 73–79. [CrossRef]
29. Shah, P.; Agashe, S. Review of fractional PID controller. *Mechatronics* **2016**, *38*, 29–41. [CrossRef]
30. Shouran, M.; Alsseid, A.M. Cascade of Fractional Order PID based PSO Algorithm for LFC in Two-Area Power System. In Proceedings of the 2021 3rd International Conference on Electronics Representation and Algorithm (ICERA), Yogyakarta, Indonesia, 29–30 July 2021. [CrossRef]
31. Muftah, M.N.; Faudzi, A.A.M.; Sahlan, S.; Shouran, M. Modeling and Fuzzy FOPID Controller Tuned by PSO for Pneumatic Positioning System. *Energies* **2022**, *15*, 3757. [CrossRef]
32. Eberhart, R. Particle Swarm Optimisation. *IEEE Int. Conf. Neural Netw.* **1995**, 1942–1948. [CrossRef]
33. Eberhart, R. A Modified Particle Swarm Optimizer. In Proceedings of the 1998 IEEE International Conference on Evolutionary Computation Proceedings. IEEE World Congress on Computational Intelligence (Cat. No.98TH8360), Anchorage, AK, USA, 4–9 May 1998. [CrossRef]
34. Solihin, M.I.; Tack, L.F.; Kean, M.L. Tuning of PID Controller Using Particle Swarm Optimization (PSO). *Int. J. Adv. Sci. Eng. Inf. Technol.* **2011**, *1*, 458–461. [CrossRef]
35. Shouran, M.; Anayi, F.; Packianather, M.; Habil, M. Different Fuzzy Control Configurations Tuned by the Bees Algorithm for LFC of Two-Area Power System. *Energies* **2022**, *15*, 657. [CrossRef]
36. Faudzi, A.A.M.; Mustafa, N.D.; Azman, M.A.; Osman, K. Position Tracking of Pneumatic Actuator with Loads by Using Predictive and Fuzzy Logic Controller. *Adv. Mater. Res.* **2014**, *903*, 259–266. [CrossRef]
37. Sulaiman, S.F.; Rahmat, M.F.; Faudzi, A.A.M.; Osman, K.; Salim, S.N.S.; Samsudin, S.I.; Azira, A.R. Enhanced position con-trol forpneumatic system by applying constraints in MPC algorithm. *Int. J. Electr. Comput. Eng.* **2017**, *7*, 1633–1642.